Variation of the gene coding for DARPP-32 (PPP1R1B) and brain connectivity during associative emotional learning

Curcic-Blake, B.; Swart, M.; ter Horst, G.J; Langers, D.R.M.; Kema, I.P.; Aleman, A.

Published in:
Neuroimage

DOI:
10.1016/j.neuroimage.2011.08.036

Publication date:
2013

NeuroImage 59 (2012) 1540–1550

Contents lists available at SciVerse ScienceDirect

NeuroImage

journal homepage: www.elsevier.com/locate/ynimg

Variation of the gene coding for DARPP-32 (PPP1R1B) and brain connectivity during associative emotional learning

Branislava Ćurčić-Blake [a,*], Marte Swart [a], Gert J. Ter Horst [a], Dave R.M. Langers [b], Ido P. Kema [c], André Aleman [a]

[a] Cognitive Neuropsychiatry Group, Department of Neuroscience, Neuroimaging Center (NIC), University Medical Center Groningen, University of Groningen, Antonius Deusinglaan 2, 9713 AW Groningen, The Netherlands
[b] Department of Otorhinolaryngology, University Medical Center Groningen, University of Groningen Hanzeplein 1, 9700 RB Groningen, The Netherlands
[c] Department of Laboratory Medicine, University of Groningen, University Medical Center Groningen, Hanzeplein 1, 9700 RB, Groningen, The Netherlands

ARTICLE INFO

Article history:
Received 4 March 2011
Revised 1 August 2011
Accepted 11 August 2011
Available online 19 August 2011

Keywords:
Dynamic causal modelling (DCM)
Associative emotional learning
Dopamine
Genetics
DARPP-32
Effective connectivity

ABSTRACT

Associative emotional learning, which is important for the social emotional functioning of individuals and is often impaired in psychiatric illnesses, is in part mediated by dopamine and glutamate pathways in the brain. The protein DARPP-32 is involved in the regulation of dopaminergic and glutaminergic signaling. Consequently, it has been suggested that the haplotypic variants of the gene PPP1R1B that encodes DARPP-32 are associated with working memory and emotion processing.

We hypothesized that PPP1R1B should have a significant influence on the network of brain regions involved in associative emotional learning that are rich in DARPP-32, namely the striatum, prefrontal cortex (comprising the medial frontal gyrus and inferior frontal gyrus (IFG)), amygdala and parahippocampal gyrus (PHG). Dynamic causal models were applied to functional MRI data to investigate how brain connectivity during an associative emotional learning task is affected by different single-nucleotide polymorphisms (SNPs) of PPP1R1B: rs879606, rs907094 and rs3764352.

Compared to heterozygotes, homozygotes with GTA alleles displayed increased intrinsic connectivity between the IFG and PHG, as well as increased excitability of the PHG for negative emotional stimuli. We have also elucidated the directionality of these genetic influences. Our data suggest that homozygotes with GTA alleles involve stronger functional connections between brain areas in order to maintain activation of these regions. Homozygotes might engage a greater degree of motivational learning and integration of information to perform the emotional learning task correctly.

We conclude that PPP1R1B is associated with the neural network involved in associative emotional learning.

Introduction

Imaging genetics provides insight into the links between brain functioning, behavior and the genetical predisposition of individuals. In psychiatry the attempts to identify genes linked with emotional processing are relevant (Aleman et al., 2008; Blasi et al., 2009; Canli et al., 2009). One such gene, PPP1R1B, encodes the phosphoprotein DARPP-32 and has been suggested to be of relevance for emotional and memory processing (Meyer-Lindenberg et al., 2007). DARPP-32 has been implicated in a number of neurological disorders such as schizophrenia (Albert et al., 2002) and depression (Svenningsson et al., 2002), as well as in drug abuse (Svenningsson et al., 2005) and addiction (Scheggi et al., 2004). The association of this gene with brain functioning remains relatively unexplored, however, Meyer-Lindenberg et al. (2007) have found evidence relating the haplotypic variants of this gene with brain activation and the connectivity of the striatum. Genetic variation in the single-nucleotide polymorphism (SNP) rs907094 of PPP1R1B has been associated with processing of anger (Reuter et al., 2009) and reward learning (Frank et al., 2007). In this study we aim to shed more light on the contribution of PPP1R1B to the neural basis of emotional processing.

Because the 32 kDa dopamine- and cAMP-regulated phosphoprotein, DARPP-32, both mediate and integrate glutamate and dopamine signaling (Fernandez et al., 2006) that have been implicated in emotional learning (Gillespie and Ressler, 2005; Greba et al., 2001) and associative learning (Breitenstein et al., 2006; Smith et al., 2006a) we chose a task of associative emotional learning to study brain activation differences influenced by variation in PPP1R1B. This choice was reasonable also because integration of glutamate- and dopamine-mediated

Abbreviations: BMS, Bayesian Model Selection; BMA, Bayesian Model Averaging; BVAQ, Bermond–Vorst Alexithymia Questionnaire; DCM, Dynamic Causal Model; GLM, General Linear Model; IFG, Inferior frontal gyrus; MFG, Medial frontal gyrus; RFX, Random effects analysis; VOI, Volume of Interest.

* Corresponding author. Fax: +31 503638875.
E-mail address: b.curcic@med.umcg.nl (B. Ćurčić-Blake).

1053-8119/$ – see front matter © 2011 Elsevier Inc. All rights reserved.
doi:10.1016/j.neuroimage.2011.08.036

signals is required for the induction of synaptic plasticity, long-term memory (Calabresi et al., 2007; O'Carroll et al., 2006), long-term potentiation (O'Carroll and Morris, 2004), and learning (Baldwin et al., 2002; Smith-Roe and Kelley, 2000).

DARPP-32 was found in neurones with dopamine receptors D1 and D2 with the highest concentrations in the striatum (which comprises the putamen and caudate) and the olfactory tubercle and moderate levels in the amygdala, hippocampus and prefrontal cortex (PFC) (Ouimet et al., 1992). These regions overlap with brain regions implicated in associative learning of emotional words and pictures from our previous study (Curcic-Blake et al., 2011): amygdala, inferior frontal gyrus (IFG) and medial frontal gyrus (MFG) are implicated when emotional stimuli were compared with neutral stimuli, and parahippocampal gyrus (PHG) and putamen for all stimuli. Similarly, Sperling and colleagues established that the hippocampus, PHG, IFG, MFG, caudate, fusiform and superior parietal cortices are activated during associative learning of novel as opposed to repeated face and name pairs (Sperling et al., 2001).

Because DARPP-32, promotes cell signaling by inhibiting PP1 (Hemmings et al., 1984), one may expect that genetic variations of the DARPP-32 encoding gene would influence certain signalling pathways in the human brain. This could be mediated, for example, by different gene expressions or by a difference in protein excitability for two different genotypes. As yet, only one study addressed this question. Meyer-Lindenberg et al., (2007) have shown that the homozygotes of a common haplotype exhibit both greater activation in the putamen and increased functional connectivity between the dorsolateral PFC (DLPFC) and putamen during emotional processing and working memory tasks.

Therefore, we predicted that the homozygotes GTA of the haplotype on SNPs rs879606, rs3764352 and rs907094 present stronger effective connectivity between the left PFC and the medial temporal lobe (MTL) during associative emotional learning. To explore this hypothesis, we investigated the influence of the genotype of the GTA haplotype on the effective connectivity between the IFG, MFG, putamen, amygdala and PHG during a task that involves the association and memorization of emotional word and picture pairs.

Methods

Experimental procedure

The experimental procedure that we used has been described in detail elsewhere (Curcic-Blake et al., 2011). In short, forty students (fourteen males and twenty six females) participated in this study. The subjects were chosen from a sample of 400 university students using the Bermond–Vorst Alexithymia Questionnaire (BVAQ). In particular, the verbalizing scale of the BVAQ was used as a guideline for the inclusion of individuals with sufficient variability in their emotional verbalizing ability. During fMRI scanning an emotional (positive, negative and neutral) picture (International Affective Picture System- IAPS) and a word were displayed for 3 s. The word valence was matched to the picture valence in the sense that a negative picture (for example, a snake) was paired with a word with a negative meaning (for example, cancer). However, the semantics of the word was arbitrary, that is, it was not directly associated with the target IAPS picture. The pictures randomly included people, animals, houses and landscapes. The subject was instructed to decide whether the word and picture fitted together and to remember them. A fixation cross was then presented on the screen for a period of 2–8 s (jittered).

A recognition memory test was performed afterwards. It consisted of the same pictures as those shown in the scanner, but now presented in random order and with three words displayed beneath each picture (also ordered randomly): (1) the word that was paired with the picture (the correct answer); (2) a word semantically related to the paired word; (3) an unrelated word. The subject was asked to choose the correct answer by pressing 1, 2 or 3. The memory test was further evaluated calculating mean accuracy as well as accuracy between two genotype groups using *t*-test. The effect of emotions on the memory accuracy was determined by performing repeated measures ANOVA with valence as a within-subject measure and genotype for between subject measure.

Genotyping

EDTA anti-coagulated blood was collected from all subjects to investigate the DARPP-32 rs879606, rs3764352 and rs907094 genotype. These SNPs of the DARPP-32 encoding gene PPP1R1B are known to be associated with cognitive processing and emotions such as anger. The common haplotype of PPP1R1B has been descibed previously (Meyer-Lindenberg et al., 2007) and consists of particular variations on 7 SNPs (Table 1). DNA was isolated from EDTA anticoagulated blood using an automated DNA isolation system (X- tractor, Westburg, Leusden, The Netherlands) and the Sigma DNA isolation kit (Sigma, Zwijndrecht, The Netherlands). DARPP-32 genotypes were determined with allelic discrimination on an Applied Biosystems 7500 real-time polymerase chain reaction (PCR) system (Applied Biosystems, Nieuwekerk a/d IJssel, The Netherlands) using pre-developed assays and according to the protocol supplied by Applied Biosystems (rs879606: C___3194815_10; rs12601930: C__31016495_10; rs907094 C___7452370_1_; rs3764352: C__27480385_10). We define the major alleles for those four SNPs as G, C, T and A respectively. We determined the variations on 4 SNPs. However, because of the high frequency of the common haplotype (73%) and two other haplotypes (14% and 3.5%), we depicted the homozygotes with alleles GTA (see Table 1) of the SNPs rs879606, rs3764352 and rs907094 (Meyer-Lindenberg et al., 2007). To relate our results with previous studies, we compared the brain connectivities of two groups of subjects. The first group consisted of homozygotes with the same combination of SNPs as a common haplotype (namely the homozygotes of the GTA haplotype). The second group were heterozygotes with any other combination of these SNPs that we found. We note here that we use different labeling of the base-pair complements than Meyer-Lindenberg et al. (2007) due to our different definition of the major alleles.

Functional magnetic resonance imaging data acquisition and analysis

A 3 T Philips Intera MRI scanner (Philips, Best, The Netherlands) was used to acquire the images. Whole-brain echo-planar functional images (EPIs) were acquired using a standard 8-channel SENSE head coil. Thirty-nine axial slices were acquired with the following parameters: TR 2000 ms; TE 28 ms; flip angle 70°; SENSE factor 2; field of view 224 mm; matrix 64×62; slice thickness 3.5 mm with no slice gap, yielding voxels of 3.5×3.5×3.5 mm in size. In order to co-register and normalize the functional data, T1-weighted anatomical images were acquired: using a 3D/FFE/CLEAR sequence (TR = 25 ms, TE = 4.6 ms, flip angle = 30°, FOV = 256 mm, matrix 256× 256 mm, slice thickness 1.0 mm).

The collected magnetic resonance data in the form of 4-dimensional (4-D) volumes were first converted to 3-D files using the MRIcro software, then processed using the statistical parametric mapping program SPM8 (www.fil.ion.ucl.ac.uk/spm). The functional images were corrected for slice timing acquisition as part of the preprocessing procedure and then realigned to the first functional image. The T1-weighted images were co-registered to the mean EPI image. Low-frequency signal drift was corrected for by applying a high-pass temporal filter with a cut-off of 250 s. The co-registered data were subsequently normalized onto the MNI template and the resulting normalization parameters were applied to all the EPI images. The functional data were spatially smoothed using a 6 mm isotropic Gaussian kernel before the statistical analysis was performed.

Table 1
Genotyping results. *The common haplotype as determined by Meyer-Lindenberg et al. (2007). Note that we use different labeling of the base-pair complement than in the reference above, in accordance with the latest literature on DARPP-32 (Albert et al., 2002; Ishikawa et al., 2007); see also comments in the Materials section of Frank et al. (2009).

	rs4795390	rs879606	rs11651497	rs907094	rs3764353	rs3764352	rs3794712	Num subj.
Common haplotype *	C	G	C	A	C	T	C	
Homozygote		G/G		T/T		A/A		22
Heterozygote Type I		G/A		T/C		A/G		13
Heterozygote Type II		G/G		T/C		A/G		5

A hemodynamic function convoluted with the timings for each condition was used in the general linear model (GLM) together with an actual measured signal in order to estimate for each voxel the parameters corresponding to the contribution of each condition to the rise in signal for each subject. Two contrasts were performed for each subject, using a *t*-test: 1.) to compare the activation for the positive (P) + negative (N) emotional condition versus the neutral (n) condition (P + N > n); 2.) to compare the activation for the positive (P) + negative (N) emotional condition + the neutral (n) condition (P + N + n). The results obtained for each subject were used in the random effects analysis (RFX) to make the group inferences. In order to investigate the process of associative learning, we analyzed both successfully and unsuccessfully memorized trials.

Volumes of interest

There is evidence that emotional learning involves an assembly of the medial temporal lobe (including the hippocampus and parahippocampal gyrus), striatum, medial and dorsolateral prefrontal cortices, and amygdala (Delgado et al., 2008; Depue et al., 2007; Kensinger and Corkin, 2004; Kilpatrick and Cahill, 2003; LeDoux, 1996; McGaugh et al., 1996; Peper et al., 2006; Phelps, 2006; Phelps and LeDoux, 2005; Richter-Levin, 2004; Sperling et al., 2001). The RFX maxima from the two contrasts served as the basis for time-course extraction for the dynamic causal modeling (DCM) analysis. First, the anatomical regions were extracted from 'TD labels' (for the MFG, PHG and IFG) and 'aal' maps (for the putamen and the amygdala) from wfu_pickatlas (Maldjian et al., 2003, 2004; Tzourio-Mazoyer et al., 2002). The guiding coordinates were defined to coincide with the maximum RFX activation voxel for the MFG, IFG and amygdala (contrast P + N > n) and for the putamen and PHG (contrast P + N + n) within their anatomical regions. We continued our analysis using the volumes of interest (VOIs) in the left hemisphere, where a well known area of the brain associated with language, Brocca's area (BA 44/45 our left IFG), is situated.

The centre of the VOI for each subject was then defined as the maximum activation (P + N vs n contrast, $p<0.05$, uncorrected) in the given region, close to the RFX maximum (cut-off at 16 mm) and still belonging to the same anatomical region (visual inspection). Finally, 4 mm radius spheres were drawn around the center defined above, and time series of the activated voxels within the sphere were extracted while their first principal component was simultaneously calculated. The first principal component was used for further connectivity analysis.

Dynamical causal models—the model space

Our aim was to investigate the differences in the connectivity between the PFC and the putamen, and between the PFC and the PHG for two genotype groups. The dynamical causal modeling (DCM) option in SPM8 (Friston et al., 2003) was used to evaluate the effective connectivity between the MFG, IFG, amygdala, putamen and PHG. DCM models the observed fMRI time series of given regions as a bilinear dynamic interaction on the neuronal level by incorporating the hemodynamic balloon model (Buxton et al., 1998; Stephan et al., 2007). A predefined DCM model is created and then compared with the measured data; the parameters of the model are adjusted by means of iterative Bayesian parameter estimation such that negative free energy of the model is maximized. The free energy represents a lower bound on the log model evidence, a measure of the balance between the model fit and model complexity, and is a useful objective function in order to avoid overfitting. For our purpose, several models were created, defining the Model Space, and each model was estimated separately. As a result, the so-called log evidence (free energy) was calculated for each estimated model. The models were compared using Bayesian model selection (Penny et al., 2004) using a random effects implementation for the group level, as described by Stephan et al.(2009). In short, a probability density is estimated on the models themselves by treating the model as a random variable and estimating the parameters of a Dirichlet distribution that describes the probabilities for all models considered. The likelihood that a specific model generated the data of a randomly chosen subject and the exceedance probability of one model being more likely than any other model are estimated.

The next step was to obtain an average of all models in the model space. The Bayesian model averaging (BMA) method (Penny et al., 2010) computes parameters within a model space such that more weight is given to models with higher posterior probablity, according to Bayes' rule. Those models for which the probability was very low (less than 1/20 of the maximum probability) were excluded from the calculations. This "Occam's window" approach produces approximately the same results as averaging over all models but at a fraction of the computational cost. Each DCM model consisted of the following parameters: 1. the strength of the connections between pairs of regions (referred to as directional connectivities and denoted by coefficients A); 2. the strength of modulation of the connection by a certain external input or condition (known as modulatory effects and denoted by coefficients B); 3. the direct influences of the external input or condition on the region (known as driving inputs and denoted by coefficients C). The posterior distributions for these parameters for the average model were calculated by drawing samples from a multinomial distribution of posterior beliefs for given models within subjects using a Gibbs sampling approach (Penny et al., 2010). Finally, posterior means and exceedance probabilities (that the given parameter is larger than zero) were obtained.

Our aim was to look for specific differences among coupling parameters. There is evidence from anatomical studies that all the regions considered are bidirectionally connected, either directly or via the thalamus (Amaral and Price, 1984; Haber, 2003; Vogt and Pandya, 1987). Therefore, we assumed all the effective connectivities between all 5 regions (Fig. 1a) and we varied only the modulatory influences.

The choice of input regions was determined by considering our previous study in which the emotional aspects of these tasks were investigated (Curcic-Blake et al., 2011). A model comparison of the connectivity pattern between the IFG, MFG and amygdala amygdala revealed best fit for input of emotional stimuli at the IFG. Therefore, in the current analysis we only considered models in which the emotional stimuli enter the circuitry via the IFG. We also considered that the putamen may receive both emotional and neutral stimuli; this area is known to receive inputs from many sensory and higher cognitive regions, and is important in decision making during cognitive and emotional tasks. Furthermore, the PHG is directly connected with the visual cortex

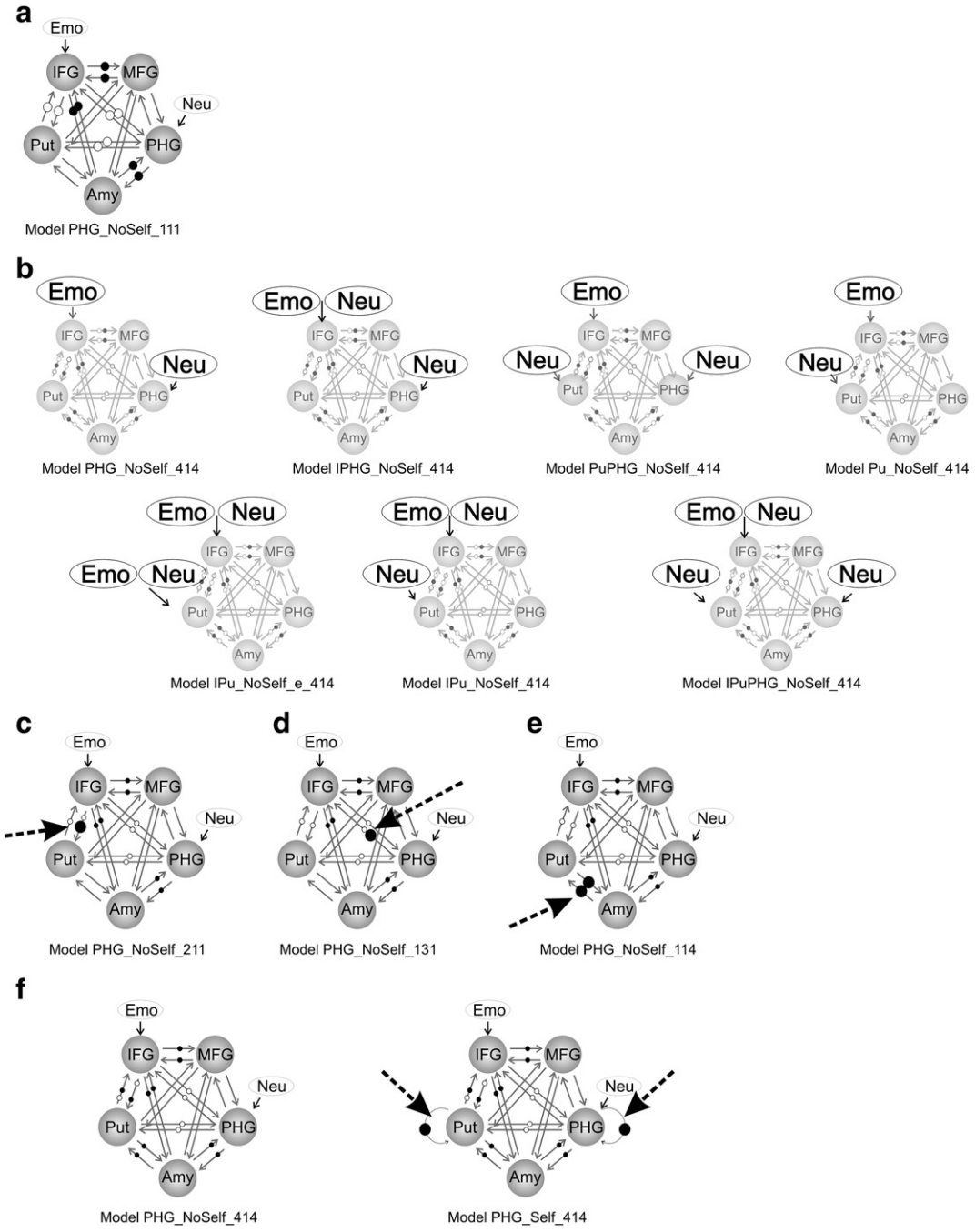

Fig. 1. Illustration of the created DCMs. a) Illustration of the basic model with modulatory connections based on the literature. All the modulatory connections from this model are present in all the models. The modulatory effect of neutral stimuli (white circles) is the same for all DCMs. b) Illustration of variations in inputs. c–e) Illustration of models chosen by systematic changes of the modulatory effects of emotional stimuli (black circles). c) Example of a model where the modulatory effects on the connections between the IFG and putamen were varied. These variations deliver 4 different families of models according to which connection is modulated: 1. none (a); 2. forward (c); 3. backward (d); 4. both (e) . This also delivers 4 families of models. e) Permutations of the modulatory effects for the putamen to the amygdala. f) Example of a model with modulatory effects on self-connections. These effects were either both icluded, or both omitted. The models not shown are linear combinations of those illustrated in a) –f); for example, model IPHG_Self_133 has the same emotional modulatory influences between the IFG and PHG as model PHG_NoSelf_131, the same between the putamen and amygdala as PHG_NoSelf_113, the same modulatory effects on self-connections as PHG_Self_114, and the same inputs as model IPHG_Self_414. In total, 896 models per subject were created.

(Blatt et al., 2003) and is thus engaged in the convergence of episodic and declarative information as well as in the formation of associative links and the making of associations (Eichenbaum, 2000), regardless of emotional context. Therefore, we allowed neutral stimuli input via the PHG. As presented in Results section, the above considerations are consistent with the brain activation pattern during the task performance for all three types of stimuli. We thus created DCMs containing combinations of the IFG, PHG and putamen as input regions. This selection produced 16 different models, of which 2 were excluded because they did not have any input region for neutral stimuli. To examine the differences between coupling and modulatory parameters, we systematically varied the modulatory effects (see below) by calculating 128 models per input combination. Since the input is of relatively lower importance, we chose 7 representative combinations of inputs (Fig. 1b) instead of calculating 14*128 models, which is computationally intensive and produces a lot of redundant models.

Based on our previous study (Curcic-Blake et al., 2011) and other connectivity studies investigating emotional memory (Smith et al.,

2006b), for all models we fixed the modulatory influences of the emotional stimuli to the connections IFG–MFG, IFG–amygdala, and amygdala–PHG in both directions. Because both the IFG and amygdala are strongly engaged in the emotional aspects of this task, the model space was created in order to question whether the emotional stimuli further modulate the connectivities IFG–putamen, IFG–PHG, and putamen–amygdala (Fig. 1c–e). The first numeral of the model number denotes the modulatory effect on the connections from the IFG to the putamen, the second numeral denotes the IFG to PHG modulatory effect (Fig. 1e). Variations of the modulatory effects for the putamen to the amygdala are denoted by the third numeral of the model number. The emotional stimuli could either: 1. not affect of the connection additionally (Fig. 1a); 2. affect the forward connection (Fig. 1c); 3. backward connection (Fig. 1d) or 4. affect the connection in both directions (Fig. 1e). Combined, the various variants give rise to 4^3 (three different connections and 4 different possibilities) different combinations of modulatory effects, thus 64 different models. Furthermore, the PHG and putamen were equally activated during emotional and neutral stimuli. We thus investigated whether the activation in these regions is stimulus independent or due to self-regulatory mechanisms by creating models with and without self-regulatory parameters. This resulted in two different possibilities denoted as _Self and _NoSelf in the model name (Fig. 1f).

In total, 7 (number of input combinations) × 64(modulatory effects on connections) × 2(self-connection yes-no) = 896 models per subject were created. Because this model set for each subject is large, many combinations of inputs with modulatory effects are possible. We divided this large model space into 4 families (see below) and then used Bayesian model averaging over a large number of models to obtain posterior estimates that do not depend on a single best model. Thus, the entire set was subdivided into families by considering whether they had a complex set of inputs (four inputs or more), or a more modest set (three inputs or less), and either a complex (5 or more) or modest (up to 4) set of modulatory effects. To statistically evaluate the posterior distribution differences, we used a bootstrapping procedure. In short, we randomly chose a sample (out of 10000) from both groups and calculated the difference, a procedure that was repeated 10,000 times to obtain the distribution of differences. The percentage of difference samples represents the probability that the difference between two groups for a particular parameter is larger than zero.

Results

Genetic results

The results of the blood test are presented in Table 1. We determined the genetic variation on the rs879606, rs3764352 and rs907094 SNPs. The genotype frequencies of all SNPs were in Hardy–Weinberg equilibrium (rs879606 - G/G:27 (67.5%), G/A: 13 (32.5%), A/A: 0 (0%); $\chi^2 = 1.51$, d.f. = 1, n.s.; rs3764352-G/G:22 (55%), G/A: 18 (45%), A/A: 0 (0%); $\chi^2 = 3.37$, d.f. = 1, n.s; rs907094-T/T: 22 (55%), T/C: 18 (45%), C/C: 0 (0%); $\chi^2 = 3.37$, d.f. = 1, n.s.). There were 22 homozygotes with the expression GTA on the above three SNPs. These overlap with the common haplotype defined by Meyer-Lindenberg et al. (2007). We also identified two types of heterozygotes on the common haplotype, which correspond to the heterozygotes of the second and third haplotypes defined by Meyer-Lindenberg et al. (2007). In order to enable a comparison with previous studies, and for further analysis, we divided our subjects into two groups: homozygotes of the common haplotype (T) and the rest—two types of heterozygotes (T/C) (see Table 1).

Memory results

Thirty-nine out of forty subjects performed uniformly well in the memory test, with a mean accuracy of 95% ± 6% (M ± SD; $n = 39$). One subject performed poorly, scoring 42% correct, and was excluded from further analysis. After performing ANOVA corrected for multiple comparisons we found an effect of valence $F(2, 38) = 3.74$, $p = 0.038$ (after the Greenhouse–Geisser sphericity correction). Accuracies for the various trials are given in Table 2. The planned contrast (Table 3) revealed a difference in the accuracy of performance between emotional and neutral trials ($p = 0.031$, $n = 39$). Both heterozygotes (96% ± 2%, $n = 17$) and homozygotes (94% ± 7%, $n = 17$) performed well in the memory test, with no significant difference between them either in total accuracy or emotional effect.

RFX fMRI results

The group activation by conventional voxel-based analysis during the ASSOCIATIVE EMOTIONAL LEARNING TASK is depicted in Fig. 2a and Table 4. Random effects GLM analysis of the emotional versus neutral condition ($p < 0.05$, FWE) revealed activation of the bilateral AMY, IFG, MFG, fusiform gyrus (visual processing area), middle temporal gyrus, superior temporal gyrus, superior frontal gyrus, caudate and posterior cingulate, and decreased activation in the inferior parietal lobule. In addition, the bilateral PHG and putamen were activated in RFX GLM analysis of the emotional + neutral contrast ($p < 0.05$ FWE).

Fig. 2b and Table 5 present the differences in group activation between the homozygotes (T) and heterozygotes (T/C) revealed by conventional voxel-based analysis during the ASSOCIATIVE EMOTIONAL LEARNING TASK. No significant differences were observed after the correction for multiple comparisons. Furthermore, according to the study on emotional processing (Meyer-Lindenberg et al., 2007), differences in the activation of the putamen and IFG might be expected. Therefore, we performed ROI analyses on these regions. After small volume corrections were made, we found no significant difference between the two groups in these regions.

Connectivity results

Regarding the VOIs, we found significant activation in all five regions in 28 subjects. Both the T and T/C groups consisted of 14 subjects. The BMS (Fig. 3a–c) method revealed that models with fewer inputs were favored for both groups (exceedance probability of 99.7% for T and 99.3% for T/C). From the entire set of 896 models, the model with the highest exceedance probability for homozygotes was IPGH_Self_121 (25.2%) and for heterozygotes was IPHG_Self_e _141 (21.8%). After dividing this entire set of 896 models into families based on input complexity (i.e., few and many inputs) and on the complexity of the modulatory influences, the BMS revealed that that the best family for both groups contained fewer inputs and many modulatory coefficients (exceedance probability of 89.1% for homozygotes and 75.7% for heterozygotes). Again, the best models differed (model IPHG_Self_341 for the T/C group with an exceedance probability of 15.67% and model IPHG_Self_342 for the T group with an exceedance probability of 23.7%). These differences in models within the group arise from a different partition of the models into families (Stephan et al., 2009). While the exceedance probabilities above may not appear to be extremely high, one should consider that they sum to one over all models considered and thus tend to decrease in magnitude as the size of the model space increases. Furthermore, there is a group of models that are

Table 2
Memory test results, showing accuracy in recognition for each type of stimulus.

Stimuli type	Mean	Std. Deviation	*N*
Negative	.96	.06	39
Positive	.96	.06	39
Neutral	.93	.10	39

Table 3
Planned contrast for memory test results.

Emotions	*df*	*F*	Sig.
Positive vs. negative	1	0.3	0.57
Neutral vs. emotional	1	5.05	0.03

similar in model evidence, which implies that BMA is the most suitable method to look for differences in connectivity strengths.

The BMA analysis revealed that the posterior parameter distributions differ for the two groups, as summarized in Tables 6, 7 and 8. We found a very significant difference between the two groups with respect to the connectivity strength from the IFG to the PHG (98% of samples showed a difference). Both the BMA results calculated from all the models and the winning two families differ slightly, and our main finding of a difference in connectivity between the IFG and PHG is independent of the set of models over which it was calculated. Furthermore, we found a tendency towards differences for the following parameters: 1. the modulatory effect of negative stimuli on the connection from the IFG to the PHG (88% of samples showed a difference); 2. the self-regulation of the PHG for negative stimuli (80% of samples showed a difference). In all three cases the values of the connectivity parameters in group T were higher than in group T/C. Examples of these parameter distributions are given in Fig. 3d. Fig. 4 summarizes the significant and moderately significant differences between the groups.

Discussion

The main finding of our study is that variation in the DARPP-32 encoding gene – PPP1R1B – is significantly associated with the functional connectivity within network of brain regions that are involved in associative emotional learning. This is specifically manifested by a difference in the intensity of effective brain connections between homozygotes and heterozygotes of the GTA haplotype. Because DARPP-32 is a major integrator of dopaminergic and glutaminergic signaling, and both associative and emotional learning involve glutaminergic and dopaminergic circuitry and interaction, we hypothesized that the variation of the DARPP-32 gene will influence this circuitry. Our findings are consistent with our original hypothesis. These findings contribute to a better understanding of the influence of the DARPP-32 encoding gene on brain functioning, and also extend our knowledge regarding the important and complicated function of the DARPP-32 protein.

We observed that the intrinsic connectivity from the IFG during associative emotional learning is higher in homozygotes of the GTA haplotype than in heterozygotes. This is consistent with the findings of Meyer-Lindenberg et al. (2007), who found that the functional connectivity between IFG and putamen is increased during both working memory tasks and emotional processing tasks in homozygotes of the common haplotype. We extend these findings by determining the directionality of the connectivity: in particular, we show that the connectivity from the IFG to the PHG is higher in homozygotes. We were able to demonstrate this by using DCM combined with BMA. Our results suggest that the homozygotes of the GTA haplotype exhibit increased connectivity from the IFG to the PHG. Because both verbal and memory centers are engaged during associative emotional learning, and DARPP-32 is expressed in both the IFG and PHG, its genotype may be expected to influence the coupling between the IFG and the PHG. Indeed, our results are in agreement with this hypothesis. The IFG to PHG connections are involved in episodic memory, the regulation of emotional–motivational states (Grady et al., 2003; Meyer-Lindenberg, 2009), and the recognition of pictures and words (Grady et al., 2003). In this light, our results might indicate that emotional–motivational states may be involved to a stronger extent in homozygotes during this task.

By calculating the BMA of the particular subsets of all models involving input to the putamen, we found a difference in the connectivity between the IFG and the putamen (Supplementary Table), similar to the study of Meyer-Lindenberg et al. (2007). This difference is not evident in the whole set of models that we used, whereas the difference in connectivity between the IFG and PHG occurs for all of the

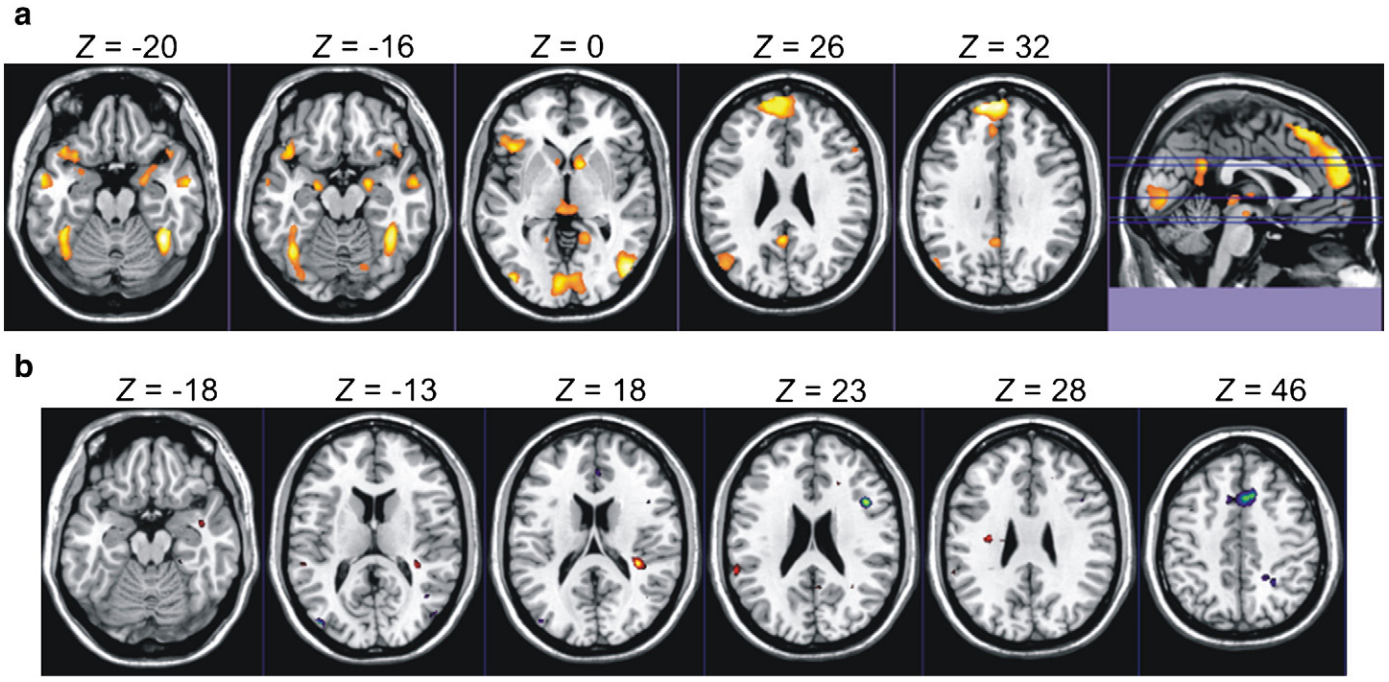

Fig. 2. Results of the RFX analysis. a) Group results for all thirty-nine subjects. Emotions (positive + negative) vs. Neutral stimuli, $p<0.05$, FWE. b) Group differences between homozygotes and heterozygotes of the GTA haplotype. Red areas: ALT emotional and neutral—homozygotes>heterozygotes in (left to right) temporal pole, STG, insula, inferior parietal lobe, PHG. Green areas: ALT emotional vs neutral—heterozygotes>homozygotes in (left to right) IFG, MFG/cingulate/SMA and parietal lobe.

Table 4
Results of conventional analysis. Random Effects (RFX), emotional>neutral. The columns list (from left to right) the chosen centers of the VOI sphere close to the highest activated voxel within the region of interest, the Brodmann area, the *MNI* coordinates, and the *Z*-score at that point.

			p<0.05 FWE T>5.72			
	BA	*x*	*y*	*z*	*Z*	*k*
Positive + negative vs neutral						
Amygdala L		−20	−8	−14	5.45	12
Amygdala R		20	−6	−16	5.52	35
Medial/superior frontal gyrus L and R	BA 10/9/8/6	−12	56	32	7.3	1478
Inferior Frontal/superior temporal gyrus R	BA 47	44	24	−14	5.37	17
Inferior/superior frontal gyrus L	BA 45/47/38/11	−42	30	−10	6.03	333
Fusiform gyrus L	BA 37	−40	−60	−16	6.38	113
Fusiform gyrus R	BA 37	38	−50	−20	7.33	202
Middle/inferior temporal L	BA 21/20	−58	0	−22	5.7	55
Middle/inferior temporal	BA 21/20	58	−4	−18	5.61	38
Occipital R	BA 39/19/37	48	−72	4	7.29	881
Occipital L	BA 39/19/22	−50	−74	12	6.99	684
Lingual R	BA 18/19	12	−82	−10	5.32	38
Lingual L and R	Ba 17 L/18 L/18R	−8	−84	4	5.96	236
Caudate R		12	10	0	5.87	25
Posterior cingulate g./cingulate g./precuneus L&C	BA 31/23	−2	−52	26	5.61	30
Posterior Cingulate/Parahippocampal gyrus	BA 30/19/29	14	−50	2	5.37	47
Neutral vs Positive + Negative						
Inferior parietal Lobule R/postcentral gyrus	BA 40	44	−36	44	5.83	184
Inferior parietal lobule R		34	−38	24	5.66	15
Middle occipital gyrus		−32	−56	−2	5.43	48
			p<0.05 FWE T>5.70			
	BA	*x*	*y*	*z*	*Z*	*k*
Positive + Negative + Neutral						
Parahippocampal gyrus L		−28	−32	−18	7.72	164
Parahippocampal gyrus R		20	−42	−10	Inf	266
Putamen L		−30	−6	−4	5.15	12
Putamen L		20	10	8	3.57	222
Guiding coordinates						
Amygdala L		−20	−8	−16	5.33	
Amygdala R		20	−4	−16	5.43	
Inferior frontal gyrus L	BA 47	−44	24	2	5.81	
Inferior frontal gyrus R	BA	44	24	−14	5.37	
Medial frontal gyrus L	BA 10	−6	64	20	6.61	
Medial frontal gyrus R	BA 10	6	62	18	6.25	
Putamen L		−28	−32	−18	7.72	
Putamen R		20	−42	−10	Inf	
Parahippocampal gyrus L		−30	−6	−4	5.15	
Parahippocampal gyrus R		20	10	8	3.57	

Table 5
Group differences between homozygotes (T) and heterozygotes (T/C) of the GTA haplotype. These are all uncorrected data; the differences are insignificant.

Positive + negative vs neutra	*p*<0.001 k>10					
	BA	*x*	*y*	*z*	*Z*	*k*
T>T/C						
Medial frontal gyrus		−12	54	10	4.08	10
Anterior cingulate/medial frontal gyrus	10	6	50	12	3.5	10
T/C>T						
T>/TC						
Insula / STG	13	34	−36	18	3.5	13
T/C>T						
Fusiform G/PHG	36/37	−36	−36	−16	3.6	21
Middle occipital gyrus	19	34	−88	12	4.4	59
Postcentral gyrus	2	−48	−24	48	4.1	62
Superior/medial frontal G	6	20	−16	68	4.3	46
Middle occipital/middle temporal gyrus	39/19	−46	−74	10	3.6	26
Medial frontal gyrus	6	−10	−4	56	3.8	24
Medial frontal gyrus	24	12	−10	48	3.4	22
Lingual gyrus	47	−6	−82	−2	3.6	17
Inferior frontal/middle frontal G	47	30	36	−8	3.8	13
Cuneus	18	−18	−74	14	3.4	11

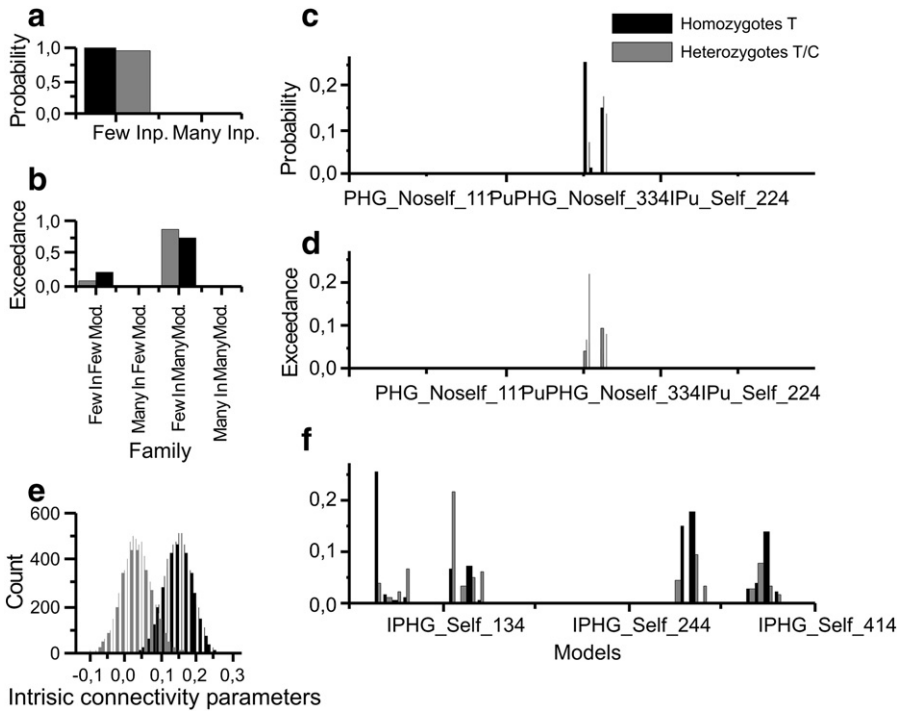

Fig. 3. BMS and BMA results. Exceedance probabilities of families (a–b) and models (c–d and f) as a result of BMS including 896 models. f) Enlarged and combined section from c) and d) of the models with highes exceedance probability. Same family "win" for the two genetic variants (homozygotes and heterozygotes of the GTA haplotype). e) Distirbutions of posterior probabilities for different parameters of connectivity as calculated by BMA. It is evident that the distributions of connectivity strengths for homozygotes and heterozygotes of a common haplotype differ from the IFG to the PHG.

subsets tested. It is possible that the use of too many models broadens the posterior distributions of the connectivity coefficient, leading to differences between groups being smeared out. Nevertheless, our results on the subsets combined with those of Meyer-Lindenberg suggest that this difference is genuine. The importance of the connection between the DLPFC and the striatum (of which the putamen is a part) is highlighted by Meyer-Lindenberg et al., being referred to as a "filter of information competing for prefrontal cortical processing". Indeed, the pathway between the putamen and IFG is involved in social recognition, reward processing, reward-guided behavior (Cohen et al., 2009) and the integration of sensimotor, cognitive and emotional information (Alexander et al., 1986). Because we observed no difference between the two genetic groups in the memory test, our results might indicate that homozygotes of the GTA haplotype employ a greater degree of sensorimotor integration to achieve the same results. The GTA genotype of the DARPP-32 encoding gene had no influence on the cognitive performance of our subjects. Both groups performed equally well in the memory recognition test and the genotype had no effect on emotional memory. Similarly, we found no significant differences (after correction for multiple comparisons) in brain activation using the GLM between the two groups. This might appear in conflict with the findings of Meyer-Lindenberg et al., who found an effect of genetic predisposition with respect to the common haplotype on working memory performance and on activation of the putamen (Meyer-Lindenberg et al., 2007). However, that study used different tasks that did not require associations to be made or explicit encoding. Similarly, the recognition test that we used after the fMRI measurement is easier to perform than the n-back task used by Meyer-Lindenberg et al., which might limit the scoring range and therefore the capacity to detect differences in performance.

Surprisingly, we found that the self-regulation term for negative stimuli of the PHG is higher in homozygotes than in heterozygotes of a GTA haplotype. The modulation of self-connection of the PHG by negative stimuli was positive for homozygotes and essentially zero for heterozygotes. This indicates that the homozygotes of the GTA haplotype employ much more self-upregulation (because those coefficients are positive) of the PHG during the storage of negative emotional stimuli. The PHG is considered to be a 'comparator' for cognitive self-monitoring (Shergill et al., 2003). In this light it appears that during the associative learning of negative word and picture pairs, the PHG in the homozygotes self-engages specially for a comparison of cognitive input with negative valence.

Table 6
Differences between posterior coefficients for the effective connectivity calculated by bootstrapping homozygotes–heterozygotes. Columns 2–4 show the percentage of sample differences for which homozygotes of a common haplotype had a higher connectivity than heterozygotes. The right-hand column shows the difference of the means of posterior parameters between homozygotes and heterozygotes.

Connectivity	All 896 models [%]	Winning family of models [%]	Mean difference for BMS on all 896 models
IFG to MFG	43.1	46.8	−0.007
Amy to MFG	52.2	52.6	0.004
Put to MFG	61.1	58.3	0.016
PHG to MFG	64.0	66.1	0.021
MFG to IFG	55.6	54.2	0.009
Amy to IFG	51.8	49.5	0.003
Put to IFG	50.2	47.1	0.001
PHG to IFG	45.8	41.8	−0.007
MFG to Amy	54.6	54.1	0.007
IFG to Amy	55.0	45.9	0.006
Put to Amy	49.6	50.3	0.000
PHG to Amy	52.5	51.9	0.004
MFG to Put	48.3	47.8	−0.004
IFG to Put	68.5	51.7	0.025
Amy to Put	55.1	51.9	0.007
PHG to Put	60.2	50.8	0.016
MFG to PHG	67.1	66.6	0.027
IFG to PHG	98.1	95.6	0.120
Amy to PHG	56.7	57.2	0.011
Put to PHG	37.9	49.5	−0.019

Table 7
Differences between posterior coefficients for the modulatory effects of positive (left), negative (middle) and neutral (right) stimuli on the connectivity, calculated by bootstrapping homozygotes–heterozygotes. Column 2 (of each table) shows the percentage of sample differences for which homozygotes of a common haplotype had higher modulatory effects on the connectivity than heterozygotes. The right-hand columns show the difference of the means of posterior parameters between homozygotes and heterozygotes.

Positive on	Probab	Mean diff
IFG to MFG	49.8	−0.001
MFG to IFG	47.1	−0.002
Amy to IFG	49.9	−0.002
Put to IFG	49.7	0.001
PHG to IFG	51.5	0.001
IFG to Amy	42.4	−0.010
Put to Amy	51.5	0.001
PHG to Amy	51.2	0.002
IFG to Put	47.7	0.001
Amy to Put	51.4	0.001
Put to Put	56.3	0.009
IFG to PHG	76.9	0.039
Amy to PHG	52.0	0.003
PHG to PHG	68.0	0.026
Negative on		
IFG to MFG	43.4	−0.009
MFG to IFG	52.7	0.004
Amy to IFG	51.7	0.005
Put to IFG	53.5	0.004
PHG to IFG	47.9	−0.003
IFG to Amy	51.2	0.003
Put to Amy	51.7	0.003
PHG to Amy	56.6	0.009
IFG to Put	51.6	0.002
Amy to Put	52.7	0.003
Put to Put	53.7	0.005
IFG to PHG	87.7	0.061
Amy to PHG	55.6	0.010
PHG to PHG	80.0	0.048
Neutral on		
Put to IFG	49.4	−0.001
PHG to IFG	55.4	0.008
IFG to Put	47.4	−0.004
PHG to Put	45.8	−0.008
IFG to PHG	57.3	0.013
Put to PHG	52.6	0.003

We have demonstrated that the observed group differences are not due to the model selection procedure, by showing that the results are independent of the models chosen to calculate the parameter differences by means of BMA (Fig. 3e). As a careful reader may notice, while creating our DCM models we did not examine all possible

Table 8
The mean and probabilities of posterior distributions for the coefficients of effective connectivities and for the modulatory effects of positive, negative and neutral stimuli on the connectivities that showed significant differences between groups. Values for homozygotes T (second and third columns) and heterozygotes T/C (fifth and sixth columns) are compared. Percent of modulatory influence was calculated by $\% = \frac{M_B}{M_A} \cdot 100$. Here, M_A is the mean of the intristic connectivity and M_B is the mean of the modulatory effect coefficient. fourth.

	T			T/C		
Concectivity	Mean	Probability [%]	Percent of modulatory influence	Mean	Probability [%]	Percent of modulatory influence
IFG to PHG	0.151	100		0.031	76	
Negative IFG to PHG	0.065	96	43	0.005	54	16
Negative on PHG to PHG	0.100	100	10	0.052	91	5

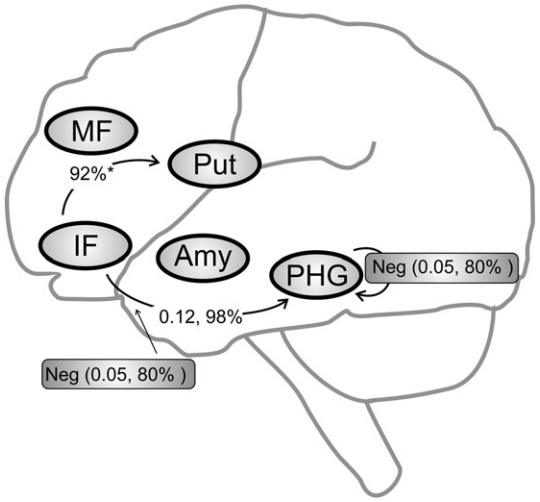

Fig. 4. Illustration of differences in connectivity parameters between homozygotes and heterozygotes of a common haplotype. The mean difference and the exceedance probability that homozygotes have stronger connectivity or modulatory effect are denoted. Both significant differences (those exceeding 90%) and differences showing a trend are depicted. The diferrence in connectivity parameters between IFG and putamen occur only in subset of models.

modulatory effects. Even though this would be a powerful exploratory method for the investigation of new effects, it would be of no benefit in answering our specific research question regarding the association of effective connectivities with the DARPP-32 genotype.

In our analysis, the time courses of the brain regions were extracted from two contrasts. This procedure was necessary because the PHG and putamen have few voxels on the group level for emotional versus neutral stimuli. Because DCM is typically used to compare different mechanistic explanations for specific activations detected by SPM, including those with different response profiles (Stephan et al., 2010), it is reasonable to choose the best contrast for the PHG and putamen. Furthermore, the hippocampal formation and the PHG have been implicated in the detection of novelty (Tulving et al., 1996); both the emotional and neutral stimuli were novel to the subjects.

How DARPP-32 genotypes affect functional connectivity is a matter of debate. It is known that the function of DARPP-32 is determined by its phosphorylation state. DARPP-32 can be phosphorylated on several sites such as Thr-34, Thr-75 , Ser-137 and Ser-102. For example, when DARPP-32 is phosphorylated at a single site Thr-34, which can be induced by the action of dopamine on the D1 dopamine receptors, it inhibits the protein phosphatase-1 (PP1) (Hemmings et al., 1984). PP1 is a major inhibitor of further cell signaling and cell excitability. In our study we demonstrate the link between genetic variations on the PPP1R1B gene encoding the DARPP-32 protein and the connectivity between regions involved in dopamine-mediated learning. It is unknown whether genetic variations affect the expression or efficiency of DARPP-32 in these regions and how this relates to neurotransmitter signaling. Evidence has been reported for a decreased concentration of DARPP-32 in the DLPFC in subjects with schizophrenia and bipolar disorder (Albert et al., 2002; Ishikawa et al., 2007). Another study (Baracskay et al., 2006) failed to find evidence for any decrease in the transcript level in the PFC of schizophrenia patients, whereas a small subject study found a reduced level of DARPP-32 mRNA in the PFC in completed suicide victims with schizophrenia (Feldcamp et al., 2008). Further investigations of the influence of PPP1R1B are inconsistent. No association of this gene with schizophrenia was observed in Chinese (Hu et al., 2007; Li et al., 2006) and Japanese populations (Yoshimi et al., 2008), but another study found that a common haplotype of PPP1R1B predicted the risk of schizophrenia (Meyer-Lindenberg et al., 2007). Furthermore,

increased functional connectivity between the hippocampus and the DLPFC was found during a working memory task in patients with schizophrenia (Meyer-Lindenberg et al., 2005). Taken together, this evidence suggests that the homozygotes of a GTA haplotype might have an altered concentration of DARPP-32 in either the DLPFC, PHG or putamen, but this is still speculative. Further investigations are required to provide insight into the gene–protein relationship.

To conclude, our results demonstrate that the DARPP-32 encoding gene is associated with brain connectivity during associative emotional learning. Abnormalities in DARPP-32 levels have been implicated in a number of psychiatric disorders and the present results may contribute to research into the neural consequences of variations in the DARPP-32 encoding gene.

Supplementary materials related to this article can be found online at doi:10.1016/j.neuroimage.2011.08.036.

Acknowledgments

The authors thank G.R. Blake, D.A.J. Dijck, M.J. van Tol and E.M. Opmeer for their comments on earlier versions of the manuscript, as well as W. D. Penny for their comments on the analysis. This research was supported by a EURYI Award from the European Science Foundation to A.A.

References

Albert, K.A., Hemmings Jr., H.C., Adamo, A.I.B., Potkin, S.G., Akbarian, S., Sandman, C.A., Cotman, C.W., Bunney, W.E.J., Greengard, P., 2002. Evidence for decreased DARPP-32 in the prefrontal cortex of patients with schizophrenia. Arch. Gen. Psychiatry 59, 705–712.

Aleman, A., Swart, M., van Rijn, S., 2008. Brain imaging, genetics and emotion. Biol. Psychol. 79, 58–69.

Alexander, G.E., DeLong, M.R., Strick, P.L., 1986. Parallel organization of functionally segregated circuits linking basal ganglia and cortex. Annu. Rev. Neurosci. 9, 357–381.

Amaral, D.G., Price, J.L., 1984. Amygdalo-cortical projections in the monkey (*Macaca fascicularis*). J. Comp. Neurol. 230, 465–496.

Baldwin, A.E., Sadeghian, K., Kelley, A.E., 2002. Appetitive instrumental learning requires coincident activation of NMDA and dopamine D1 receptors within the medial prefrontal cortex. J. Neurosci. 22, 1063–1071.

Baracskay, K.L., Haroutunian, V., Meador-Woodruff, J.H., 2006. Dopamine receptor signaling molecules are altered in elderly schizophrenic cortex. Synapse 60, 271–279.

Blasi, G., Lo Bianco, L., Taurisano, P., Gelao, B., Romano, R., Fazio, L., Papazacharias, A., Di Giorgio, A., Caforio, G., Rampino, A., Masellis, R., Papp, A., Ursini, G., Sinibaldi, L., Popolizio, T., Sadee, W., Bertolino, A., 2009. Functional variation of the dopamine D2 receptor gene is associated with emotional control as well as brain activity and connectivity during emotion processing in humans. J. Neurosci. 29, 14812–14819.

Blatt, G.J., Pandya, D.N., Rosene, D.L., 2003. Parcellation of cortical afferents to three distinct sectors in the parahippocampal gyrus of the rhesus monkey: an anatomical and neurophysiological study. J. Comp. Neurol. 466, 161–179.

Breitenstein, C., Korsukewitz, C., Floel, A., Kretzschmar, T., Diederich, K., Knecht, S., 2006. Tonic dopaminergic stimulation impairs associative learning in healthy subjects. Neuropsychopharmacology 31, 2552–2564.

Buxton, R.B., Wong, E.C., Frank, L.R., 1998. Dynamics of blood flow and oxygenation changes during brain activation: the balloon model. Magn. Reson. Med. 39, 855–864.

Calabresi, P., Picconi, B., Tozzi, A., Di Filippo, M., 2007. Dopamine-mediated regulation of corticostriatal synaptic plasticity. Trends Neurosci. 30, 211–219.

Canli, T., Ferri, J., Duman, E.A., 2009. Genetics of emotion regulation. Neuroscience 164, 43–54.

Cohen, M.X., Schoene-Bake, J.C., Elger, C.E., Weber, B., 2009. Connectivity-based segregation of the human striatum predicts personality characteristics. Nat. Neurosci. 12, 32–34.

Curcic-Blake, B., Swart, M., Aleman, A., 2011. Bidirectional information flow in fronto-amygdala circuits in humans: a dynamic causal modeling study of emotional associative learning. Cereb. Cortex. doi:10.1093/cercor/bhr124..

Delgado, M.R., Nearing, K.I., LeDoux, J.E., Phelps, E.A., 2008. Neural circuitry underlying the regulation of conditioned fear and its relation to extinction. Neuron 59, 829–838.

Depue, B.E., Curran, T., Banich, M.T., 2007. Prefrontal regions orchestrate suppression of emotional memories via a two-phase process. Science 317, 215–219.

Eichenbaum, H., 2000. A cortical–hippocampal system for declarative memory. Nat. Rev. Neurosci. 1, 41–50.

Feldcamp, L.A., Souza, R.P., Romano-Silva, M., Kennedy, J.L., Wong, A.H., 2008. Reduced prefrontal cortex DARPP-32 mRNA in completed suicide victims with schizophrenia. Schizophr. Res. 103, 192–200.

Fernandez, E., Schiappa, R., Girault, J.A., Le Novere, N., 2006. DARPP-32 is a robust integrator of dopamine and glutamate signals. PLoS Comput. Biol. 2, e176.

Frank, M.J., Moustafa, A.A., Haughey, H.M., Curran, T., Hutchison, K.E., 2007. Genetic triple dissociation reveals multiple roles for dopamine in reinforcement learning. Proc. Natl. Acad. Sci. 104, 16311–16316.

Frank, M.J., Doll, B.B., Oas-Terpstra, J., Moreno, F., 2009. Prefrontal and striatal dopaminergic genes predict individual differences in exploration and exploitation. Nat. Neurosci. 12, 1062–1068.

Friston, K.J., Harrison, L., Penny, W., 2003. Dynamic causal modelling. Neuroimage 19, 1273–1302.

Gillespie, C.F., Ressler, K.J., 2005. Emotional learning and glutamate: translational perspectives. CNS Spe.ctr. 10, 831–839.

Grady, C.L., McIntosh, A.R., Craik, F.I., 2003. Age-related differences in the functional connectivity of the hippocampus during memory encoding. Hippocampus 13, 572–586.

Greba, Q., Gifkins, A., Kokkinidis, L., 2001. Inhibition of amygdaloid dopamine D2 receptors impairs emotional learning measured with fear-potentiated startle. Brain Res. 899, 218–226.

Haber, S.N., 2003. The primate basal ganglia: parallel and integrative networks. J. Chem. Neuroanat. 26, 317–330.

Hemmings, H.C., Greengard, P., Tung, H.Y.L., Cohen, P., 1984. DARPP-32, a dopamine-regulated neuronal phosphoprotein, is a potent inhibitor of protein phosphatase-1. Nature 310, 503–505.

Hu, J.X., Yu, L., Shi, Y.Y., Zhao, X.Z., Meng, J.W., He, G., Xu, Y.F., Feng, G.Y., He, L., 2007. An association study between PPP1R1B gene and schizophrenia in the Chinese population. Prog. Neuropsychopharmacol. Biol. Psychiatry 31, 1303–1306.

Ishikawa, M., Mizukami, K., Iwakiri, M., Asada, T., 2007. Immunohistochemical and immunoblot analysis of dopamine and cyclic AMP-regulated phosphoprotein, relative molecular mass 32,000 (DARPP-32) in the prefrontal cortex of subjects with schizophrenia and bipolar disorder. Prog. Neuropsychopharmacol. Biol. Psychiatry 31, 1177–1181.

Kensinger, E.A., Corkin, S., 2004. Two routes to emotional memory: distinct neural processes for valence and arousal. Proc. Natl. Acad. Sci. U.S.A. 101, 3310–3315.

Kilpatrick, L., Cahill, L., 2003. Amygdala modulation of parahippocampal and frontal regions during emotionally influenced memory storage. Neuroimage 20, 2091–2099.

LeDoux, J., 1996. The emotional brain: mysterious underpinnings of emotional life. Simon & Schuster, New York.

Li, C.H., Liao, H.M., Hung, T.W., Chen, C.H., 2006. Mutation analysis of DARPP-32 as a candidate gene for schizophrenia. Schizophr. Res. 87, 1–5.

Maldjian, J.A., Laurienti, P.J., Kraft, R.A., Burdette, J.H., 2003. An automated method for neuroanatomic and cytoarchitectonic atlas-based interrogation of fMRI data sets. Neuroimage 19, 1233–1239.

Maldjian, J.A., Laurienti, P.J., Burdette, J.H., 2004. Precentral gyrus discrepancy in electronic versions of the Talairach atlas. Neuroimage 21, 450–455.

McGaugh, J.L., Cahill, L., Roozendaal, B., 1996. Involvement of the amygdala in memory storage: interaction with other brain systems. Proc. Natl. Acad. Sci. U.S.A. 93, 13508–13514.

Meyer-Lindenberg, A., 2009. Neural connectivity as an intermediate phenotype: brain networks under genetic control. Hum. Brain Mapp. 30, 1938–1946.

Meyer-Lindenberg, A.S., Olsen, R.K., Kohn, P.D., Brown, T., Egan, M.F., Weinberger, D.R., Berman, K.F., 2005. Regionally specific disturbance of dorsolateral prefrontal-hippocampal functional connectivity in schizophrenia. Arch. Gen. Psychiatry 62, 379–386.

Meyer-Lindenberg, A., Straub, R.E., Lipska, B.K., Verchinski, B.A., Goldberg, T., Callicott, J.H., Egan, M.F., Huffaker, S.S., Mattay, V.S., Kolachana, B., Kleinman, J.E., Weinberger, D.R., 2007. Genetic evidence implicating DARPP-32 in human frontostriatal structure, function, and cognition. J. Clin. Invest. 117, 672–682.

O'Carroll, C.M., Morris, R.G.M., 2004. Heterosynaptic co-activation of glutamatergic and dopaminergic afferents is required to induce persistent long-term potentiation. Neuropharmacology 47, 324–332.

O'Carroll, C.M., Martin, S.J., Sandin, J., Frenguelli, B., Morris, R.G., 2006. Dopaminergic modulation of the persistence of one-trial hippocampus-dependent memory. Learn. Mem. 13, 760–769.

Ouimet, C.C., LaMantia, A.S., Goldman-Rakic, P., Rakic, P., Greengard, P., 1992. Immunocytochemical localization of DARPP-32, a dopamine and cyclic-AMP-regulated phosphoprotein, in the primate brain. J. Comp. Neurol. 323, 209–218.

Penny, W.D., Stephan, K.E., Mechelli, A., Friston, K.J., 2004. Comparing dynamic causal models. Neuroimage 22, 1157–1172.

Penny, W.D., Stephan, K.E., Daunizeau, J., Rosa, M.J., Friston, K.J., Schofield, T.M., Leff, A.P., 2010. Comparing families of dynamic causal models. PLoS Comput. Biol. 6, e1000709.

Peper, M., Herpers, M., Spreer, J., Hennig, J., Zentner, J., 2006. Functional neuroimaging of emotional learning and autonomic reactions. J. Physiol. Paris 99, 342–354.

Phelps, E.A., 2006. Emotion and cognition: insights from studies of the human amygdala. Annu. Rev. Psychol. 57, 27–53.

Phelps, E.A., LeDoux, J.E., 2005. Contributions of the amygdala to emotion processing: from animal models to human behavior. Neuron 48, 175–187.

Reuter, M., Weber, B., Fiebach, C.J., Elger, C., Montag, C., 2009. The biological basis of anger: associations with the gene coding for DARPP-32 (PPP1R1B) and with amygdala volume. Behav. Brain Res. 202, 179–183.

Richter-Levin, G., 2004. The amygdala, the hippocampus, and emotional modulation of memory. Neuroscientist 10, 31–39.

Scheggi, S., Rauggi, R., Gambarana, C., Tagliamonte, A., De Montis, M.G., 2004. Dopamine and cyclic AMP-regulated phosphoprotein-32 phosphorylation pattern in cocaine and morphine-sensitized rats. J. Neurochem. 90, 792–799.

Shergill, S.S., Brammer, M.J., Fukuda, R., Williams, S.C., Murray, R.M., McGuire, P.K., 2003. Engagement of brain areas implicated in processing inner speech in people with auditory hallucinations. Br. J. Psychiatry 182, 525–531.

Smith, A., Li, M., Becker, S., Kapur, S., 2006a. Dopamine, prediction error and associative learning: a model-based account. Network 17, 61–84.
Smith, A.P., Stephan, K.E., Rugg, M.D., Dolan, R.J., 2006b. Task and content modulate amygdala-hippocampal connectivity in emotional retrieval. Neuron 49, 631–638.
Smith-Roe, S.L., Kelley, A.E., 2000. Coincident activation of NMDA and dopamine D1 receptors within the nucleus accumbens core is required for appetitive instrumental learning. J. Neurosci. 20, 7737–7742.
Sperling, R.A., Bates, J.F., Cocchiarella, A.J., Schacter, D.L., Rosen, B.R., Albert, M.S., 2001. Encoding novel face-name associations: a functional MRI study. Hum. Brain Mapp. 14, 129–139.
Stephan, K.E., Weiskopf, N., Drysdale, P.M., Robinson, P.A., Friston, K.J., 2007. Comparing hemodynamic models with DCM. Neuroimage 38, 387–401.
Stephan, K.E., Penny, W.D., Daunizeau, J., Moran, R.J., Friston, K.J., 2009. Bayesian model selection for group studies. Neuroimage 46, 1004–1017.
Stephan, K.E., Penny, W.D., Moran, R.J., den Ouden, H.E., Daunizeau, J., Friston, K.J., 2010. Ten simple rules for dynamic causal modeling. Neuroimage 49, 3099–3109.
Svenningsson, P., Tzavara, E.T., Witkin, J.M., Fienberg, A.A., Nomikos, G.G., Greengard, P., 2002. Involvement of striatal and extrastriatal DARPP-32 in biochemical and behavioral effects of fluoxetine (Prozac). Proc. Natl. Acad. Sci. U.S.A. 99, 3182–3187.
Svenningsson, P., Nairn, A., Greengard, P., 2005. DARPP-32 mediates the actions of multiple drugs of abuse. AAPS J. 7, E353–E360.
Tulving, E., Markowitsch, H.J., Craik, F.I.M., Habib, R., Houle, S., 1996. Novelty and familiarity activations in PET studies of memory encoding and retrieval. Cereb. Cortex 6, 71–79.
Tzourio-Mazoyer, N., Landeau, B., Papathanassiou, D., Crivello, F., Etard, O., Delcroix, N., Mazoyer, B., Joliot, M., 2002. Automated anatomical labeling of activations in SPM using a macroscopic anatomical parcellation of the MNI MRI single-subject brain. Neuroimage 15, 273–289.
Vogt, B.A., Pandya, D.N., 1987. Cingulate cortex of the rhesus monkey: II. Cortical afferents. J. Comp. Neurol. 262, 271–289.
Yoshimi, A., Takahashi, N., Saito, S., Ito, Y., Aleksic, B., Usui, H., Kawamura, Y., Waki, Y., Yoshikawa, T., Kato, T., Iwata, N., Inada, T., Noda, Y., Ozaki, N., 2008. Genetic analysis of the gene coding for DARPP-32 (PPP1R1B) in Japanese patients with schizophrenia or bipolar disorder. Schizophr. Res. 100, 334–341.